Remote Sensing of Environment 113 (2009) 329–334

Contents lists available at ScienceDirect

Remote Sensing of Environment

journal homepage: www.elsevier.com/locate/rse

The Yearly Land Cover Dynamics (YLCD) method: An analysis of global vegetation from NDVI and LST parameters

Yves Julien *, José A. Sobrino

Global Change Unit, Imaging Processing Laboratory (IPL), Universitat de València, Poligono La Coma s/n - 46980 Paterna, Spain

ARTICLE INFO

Article history:
Received 9 May 2008
Received in revised form 4 September 2008
Accepted 29 September 2008

Keywords:
NDVI
LST
Vegetation monitoring

ABSTRACT

NDVI (Normalized Difference Vegetation Index) has been widely used to monitor vegetation changes since the early eighties. On the other hand, little use has been made of land surface temperatures (LST), due to their sensitivity to the orbital drift which affects the NOAA (National Oceanic and Atmospheric Administration) platforms flying AVHRR sensor. This study presents a new method for monitoring vegetation by using NDVI and LST data, based on an orbital drift corrected dataset derived from data provided by the GIMMS (Global Inventory Modeling and Mapping Studies) group. This method, named Yearly Land Cover Dynamics (YLCD), characterizes NDVI and LST behavior on a yearly basis, through the retrieval of 3 parameters obtained by linear regression between NDVI and normalized LST data. These 3 parameters are the angle between regression line and abscissa axis, the extent of the data projected on the regression line, and the regression coefficient. Such parameters characterize respectively the vegetation type, the annual vegetation cycle length and the difference between real vegetation and ideal cases. Worldwide repartition of these three parameters is shown, and a map integrating these 3 parameters is presented. This map differentiates vegetation in function of climatic constraints, and shows that the presented method has good potential for vegetation monitoring, under the condition of a good filtering of the outliers in the data.

1. Introduction

Traditionally, vegetation has been monitored by remote sensing through vegetation indices, among which the NDVI (Normalized Difference Vegetation Index) is by far the most widely used. However, NDVI has been showed to be responding primarily to the highly absorbing red reflective band, thus mimicking red reflectance and saturating over forested regions, while being sensitive to canopy background variation in arid and semi-arid areas (Huete et al., 1997). Therefore, additional information is needed to complete NDVI information and palliate these drawbacks. Few attempts have been made by the scientific community to integrate additional information to vegetation monitoring, mainly through the analysis of at sensor brightness temperatures. However, since the remotely sensed data with the longest time extent is derived from the AVHRR (Advanced Very High Resolution Radiometer) sensor aboard NOAA (National Oceanic and Atmospheric Administration) satellites, and since these data are contaminated by orbital drift of the NOAA platforms, observation of vegetation index and temperature relationships have been limited to short time series (Nemani & Running, 1997), for which orbital drift can be neglected.

To this date, the relations between NDVI and land surface temperature (LST) have been studied in two different ways. The first one is related to their spatial variation, when the purpose is the determination of land surface parameters such as surface moisture or evapotranspiration; the second one is related to their temporal variation, to characterize vegetation changes. However, some of the studies carried out used LST retrieved only from sensor brightness temperatures (BT). In those cases, LST is replaced by BT in the following paragraphs.

Nemani and Running (1989) studied temporal variations of NDVI and BT in Montana, showing that this relation evolved in time. The slope between BT and NDVI was sensitive to changes in canopy resistance, identifying this slope as a useful parameter for evapotranspiration estimation. Ehrlich and Lambin (1996) built a land cover classification of Africa through principal component analysis of BT/NDVI slopes over a year of monthly data. This classification compared well with a previous classification. Schultz and Halpert (1995) studied the correlations between NDVI, BT and precipitation over the globe, evidencing a generally positive correlation, especially in the high and middle latitudes, with some subtropical areas presenting a negative correlation. They also found low correlations between NDVI and BT anomaly. Lambin and Ehrlich (1996) reviewed extensively the drivers between NDVI and BT, and described a general spatial pattern of relationships between NDVI and BT, related to land cover. They concluded that BT/NDVI slope could be used to classify land cover, and monitor land cover changes over time, when associated to seasonality information, retrieved from NDVI

* Corresponding author. Tel./fax: +34 96 354 31 15.
E-mail addresses: yves.julien@uv.es (Y. Julien), sobrino@uv.es (J.A. Sobrino).

0034-4257/$ – see front matter © 2008 Elsevier Inc. All rights reserved.
doi:10.1016/j.rse.2008.09.016

annual variations alone. Nemani and Running (1997) used BT and NDVI annual variations to build a classification over United States (later extended to the whole globe) which they validated against previous classification. They also presented an approach to characterize changes in NDVI and LST parameters, which has been used in other studies (Julien et al., 2006). Lambin and Ehrlich (1997) used the results of Lambin and Ehrlich (1996) to build a change index based on NDVI and BT to retrieve change patterns in sub-Saharan Africa, which they found to be highly erratic due to interannual climatic variability. Sobrino and Raissouni (2000) presented two methods for land cover change detection in Morocco based on NDVI and LST annual variations. Borak et al. (2000) confirmed that coarse resolution estimates of change were best related to fine resolution estimates when BT and NDVI evolutions were considered. Bayarjargal et al. (2006) compared various drought indices retrieved from satellite data over Mongolia arid regions, among which BT and NDVI ratio, and concluded that no index could be selected as most reliable, and that these indices were difficult to relate to ground observations.

As for spatial variations, Nemani et al. (1993) used remotely sensed NDVI and BT to estimate surface moisture status in western Montana (USA), observing a strong negative relationship between NDVI and LST over all present biomes (grass, crops and forests). Gillies et al. (1997) validated the estimation of surface soil water content and energy fluxes from NDVI and BT with ground measurements, leading to an accuracy around 20% in these parameters. Clarke (1997) used the combined values of NDVI and BT to detect water stress in irrigated fields. Goward et al. (2002) used Simplified Simple Biosphere model to examine LST/NDVI relationships with biophysical parameters. Near-surface soil moisture, incident radiation, plant stomatal function and to a lesser degree, wind speed were found to be the most critical parameters. Soil moisture estimates from satellite data obtained using a model derived equation showed good concordance with ground measurements. Sandholt et al. (2002) designed a Temperature-Vegetation Dryness Index, related to surface moisture status from relationships between BT and NDVI, which they validated by comparison with a hydrological model over Senegal. Hope et al. (2005) evidenced a negative linear relationship between LST and NDVI in Arctic tundra ecosystems. Wang et al. (2006) designed a method for retrieving evaporative fraction from a combination of day and night LST and NDVI with an increased accuracy. Yue et al. (2007) studied Landsat retrieved NDVI and BT over various urban classes, and showed that each class presented a different pattern of relationship, validating those parameters for urban land occupation classification. Finally, Goetz (1997) showed that the use of data with different spatial resolution led to similar results regarding spatial and temporal behavior of BT/NDVI relationship.

As a conclusion to this review, few studies have used LST coupled with NDVI for vegetation monitoring, BT parameter being generally preferred over LST because of the simplicity of its estimation. Moreover, temporal analyses of the relation between LST and NDVI have been limited to theory and classification purposes, while spatial analyses have been carried out only locally, generally to estimate biophysical parameters linked to photosynthesis. Moreover, no global analysis of the NDVI-LST relationship has ever been carried out, due to the orbital drift present in NOAA/AVHRR data, which make retrieved LST temporally incoherent.

The approach chosen in this study is to use LST and NDVI parameters as a tool for describing land covers. To this end, a dataset of LST and NDVI has been built and corrected from orbital drift, and the annual behavior of NDVI and LST has been studied. Finally, a map describing the annual behavior of NDVI and LST relationship has been built.

2. Data

This study uses GIMMS (Global Inventory Modeling and Mapping Studies) data (Tucker et al., 2005) provided by M. E. Brown of the NASA Goddard Space Flight Center (USA). This dataset has global coverage (with exception of Antarctica) from November 2000 to December 2006 time period, which corresponds to NOAA-16 and NOAA-17 activity. These data are quasi 15-day composites, and have a spatial resolution of 8 km. 8 km spatial resolution was obtained by forward mapping of the satellite data in NOAA level 1B format (Kidwell, 1998) to the output bin closest to the center location of each 8 km grid cell, and respective calibration values were applied to each channel (Vermote & Kaufman, 1995). At this resolution, land cover is mainly heterogeneous, however, assuming a good geo-referencing of the data by the GIMMS group, the observed pixels correspond to the same area. The images were then composited by the GIMMS group following the NDVI MVC (Maximum Value Compositing) technique (Holben, 1986), which means that daily NDVI images were calculated and aggregated in quasi 15 day composites by selecting the day for which maximum NDVI value is reached during each compositing period for each pixel. This reference day for the given pixel is also chosen for compositing the rest of the available channels. These data are described in details in Sobrino et al. (in press), and have been corrected from orbital drift using the method described in Sobrino et al. (in press).

3. Yearly Land Cover Dynamics (YLCD) methodology

NDVI and LST time series have been retrieved for the period November 2000 to December 2006. LST estimates have been obtained using the method developed by Sobrino and Raissouni (2000). In a first step, these data have been reprojected from continental Albers projection to global lat/lon projection. In a second step, average years of NDVI and LST have been calculated over the whole period, by averaging the data over each corresponding compositing period in order to reduce the influence of residual errors. Then, a few representative pixels have been selected for visualizing yearly trajectories of NDVI and LST parameters. These representative pixels are located in the following areas: Landes forest, in France; Atacama desert, in Chile; Sahara desert, in Lybia; Gobi desert, in China; a boreal forest, in Sweden; tropical rainforests, in Amazonia, central Africa, and Sumatra. Fig. 1 shows these trajectories.

Fig. 1 shows that arid areas (Lybia, Gobi and Atacama deserts) tend to have a vertical trajectory in the NDVI-LST feature space, while tropical rainforests (Congo, Amazonia, Sumatra) tend to have a horizontal trajectory. Other areas (Landes, Sweden) show an oblique

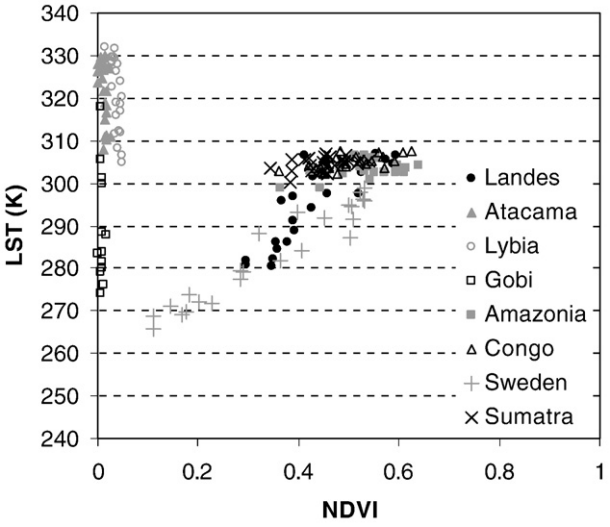

Fig. 1. Trajectories of LST-NDVI for 8 control points.

trajectory. As for yearly trajectory amplitude, Sweden shows by the far the longest, since snow presence in winter diminishes considerably NDVI and LST values. However, arid areas as well as tropical rainforests do exhibit significant yearly amplitude, limited to only one of the two parameters: NDVI for tropical rainforests, and LST for deserts.

From these trajectories, one can observe general patterns in the NDVI-LST feature space. These general patterns can be summarized with 3 parameters, which can be obtained by simple linear regression between LST and NDVI:

- the angle of the regression line with the abscissas axis,
- the length of the yearly cycle,
- the accuracy of the regression.

To obtain the yearly cycle length, we decided to project orthogonally each NDVI-LST ensemble of points on its regression line. Since orthogonal projection only makes sense in an orthonormal basis, we decided to normalize LST data between 0 and 1 as follow:

$$\hat{LST} = \frac{(LST - LST_{min})}{(LST_{max} - LST_{min})} \quad (1)$$

where $\hat{LST}$ is the normalized LST, and LST_{min} and LST_{max} are respectively the chosen minimum and maximum LST values. We have fixed LST_{min} to 240 K, and LST_{max} to 340 K. This has the advantage of setting the NDVI-LST regression line angle to the whole −90° to 90° range.

Finally, the 3 chosen parameters for description of the yearly trajectory in the NDVI-LST feature space are the following:

- θ, angle of the NDVI-$\hat{LST}$ regression line with the abscissa axis,
- d, maximum distance of the projected NDVI-$\hat{LST}$ on the regression line,
- R^2, regression coefficient, which describes the accuracy of the regression, as the rate between the variance of the regression values and the variance of the data.

These 3 parameters are presented Fig. 2. θ characterizes the relationship between NDVI and LST parameters, which is land cover dependent. For example, arid areas do exhibit little variation in NDVI while annual LST cycle can be extended ($\theta \sim \pm 90°$). Vegetation growth in semi-arid areas is limited by water availability, meaning that NDVI peak happens generally with lower temperatures ($\theta < 0°$). Temperature limited vegetation grows when temperature are higher, meaning that high NDVI values are reached for higher LST values ($\theta > 0°$). Finally, some areas see few changes in LST during the year, though NDVI values may vary ($\theta \sim 0°$). These areas correspond generally to highly vegetated areas such as rainforests. d characterizes the length of the annual cycle of the land cover. For example, areas covered with snow during winter (low NDVI and low LST) and with tall grasses (medium NDVI and medium LST) such as tundra ecosystems have a large d value, while tall grasses in savannahs for example do have a much shorter NDVI-LST annual cycle, resulting in smaller d values. Of course, the cases presented above to illustrate θ and d values are ideal cases, NDVI and LST extreme values do not coincide usually for most land covers. R^2 is a measure of the distance between ideal cases and actual land cover NDVI-LST annual behavior.

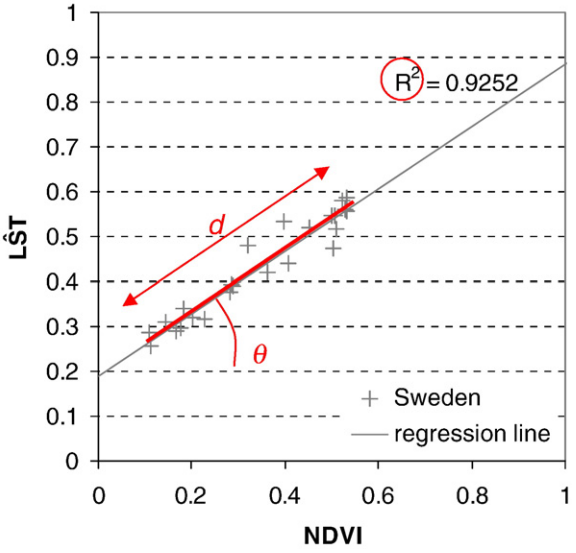

Fig. 2. Chosen parameters for vegetation description in the $\hat{LST}$-NDVI feature space.

4. Results

These 3 parameters have been retrieved for all pixels from the average year of NDVI and LST. Fig. 3 shows the spatial repartition of these parameters at global scale. As one can observe from Fig. 3a, θ gives a good description of vegetation type: arid areas tend to have vertical yearly trajectories in NDVI-LST feature space, translated in θ values greater than 70° or lower than 80°, due to a low NDVI variation throughout the year, while LST do have a yearly amplitude, result of seasonal differences in climate; semi-arid areas have negative values, showing that high NDVI values are reached at low LST values, easily explained by the fact that their vegetation is water limited and not temperature limited; tropical rainforests have θ values close to null, due to the fact that this vegetation type regulates its temperature (LST corresponding in this case to canopy temperature), maintaining it constant throughout the year, while NDVI values fluctuate depending on seasonal cloud cover (Huete et al., 2006); finally, temperate and boreal areas show a positive θ value, corresponding to high NDVI values reached for high LST values, as temperature is usually the limiting parameter for plant growth in these areas.

As regards d parameter (Fig. 3b), its repartition is simpler: areas with snow cover during winter show higher d values, since snow presence decreases both NDVI and LST values. Arid areas and tropical rainforests have little yearly amplitude in the NDVI-LST feature space, showing low d values. However, semi-arid areas have higher d values, due to the difference between NDVI values for bare soil and punctual vegetation growth, coupled with a LST yearly cycle comparable to arid areas.

As for the regression coefficient (Fig. 3c), R^2 values are close to 1 (perfect fit) for boreal and temperate areas, as well as for Sahel, North-East Brazil, Western Australia and Southern South America. R^2 values are low over deserts, due to noise in NDVI values, and over tropical rainforests. These low R^2 values over rainforests explain why some θ values in these areas are far from zero (up to 30°), evidencing residual cloud presence in the data.

Finally, Fig. 4 shows all three parameters displayed using the IHS convention: θ is coded as hue, d as intensity, and R^2 as saturation. The reasons for this choice are the following:

- θ is defined modulo 180°, meaning that angles of +90° and −90° represent the same regression line, and thus has to be coded in the same way (hue). Hue is derived from θ following Eq. (2):

$$HUE = 2*\theta - 240. \quad (2)$$

As a result, arid areas are displayed in purple ($\theta \sim \pm 90°$), semi-arid areas in yellow ($\theta \sim -30°$), evergreen forests in green ($\theta \sim 0°$) while

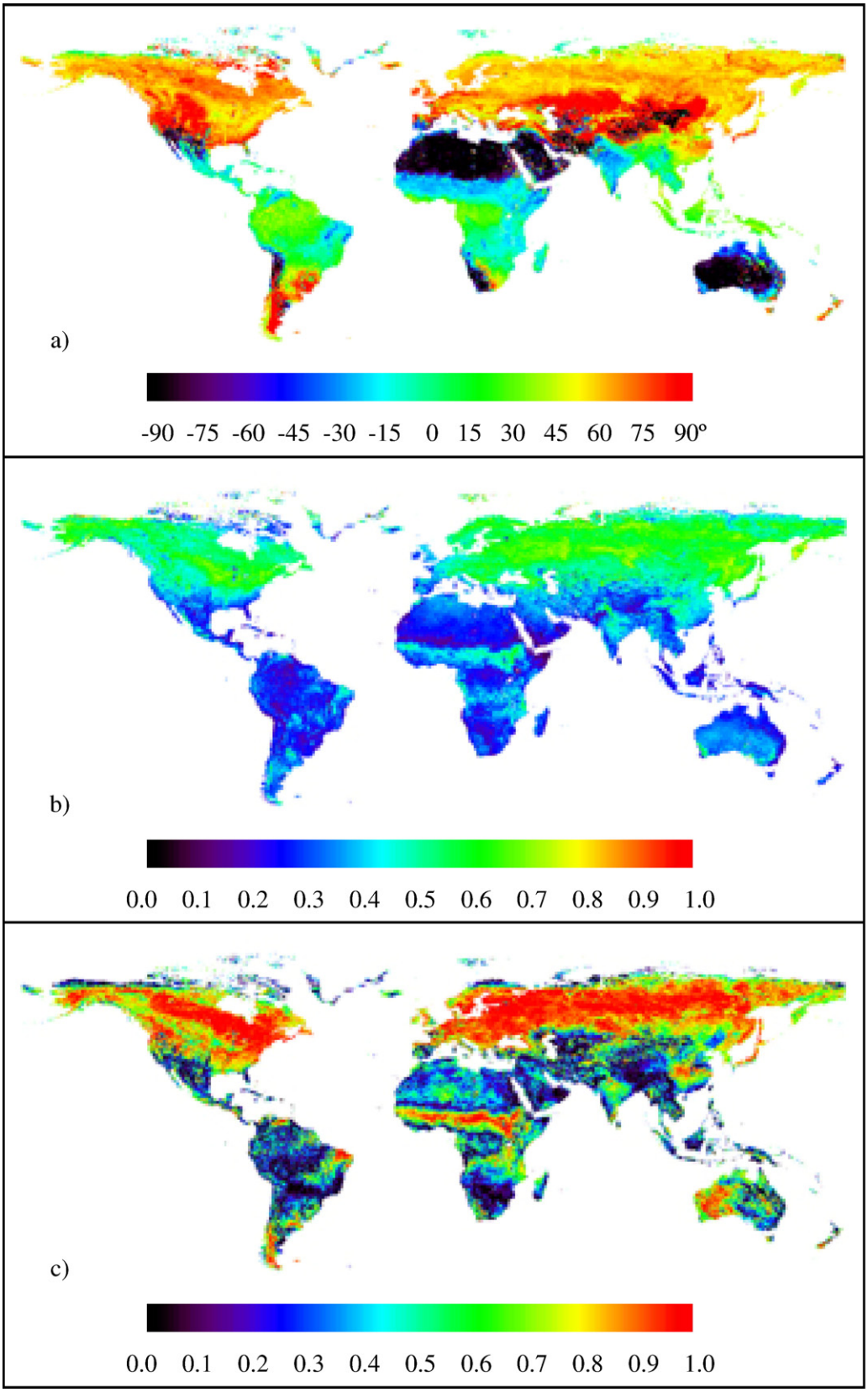

Fig. 3. Spatial repartition of a) θ (from −90° to +90°), b) d (from 0 to 1), and c) R^2 (from 0 to 1) parameters following the traditional rainbow color code.

temperate, polar, austral and mountain vegetation appear in various shades of blue (θ>0°). The code color corresponding to θ values is presented in Fig. 4.

- R^2 is relied to the confidence in the regression, which should be made clear at simple glance. To this end, saturation is a perfect tool, since low R^2 values will appear as grey, while high R^2 values

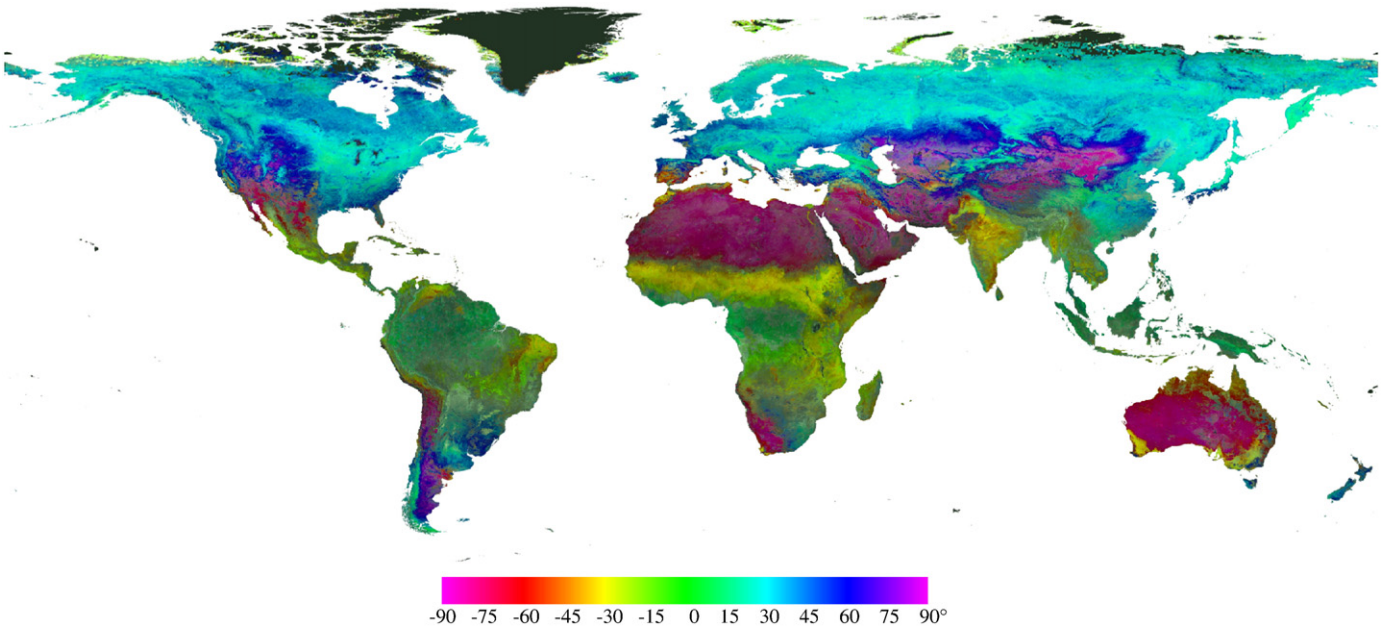

Fig. 4. IHS (Intensity–Hue–Saturation) image of NDVI-LST feature space parameter at global scale. Colors indicate θ values, characterizing vegetation types; intensity codes d values, characterizing NDVI-LST annual cycle extent; and saturation codes R^2 values, related to regression confidence.

appear in bright colors. Saturation is derived from R^2 values using Eq. (3):

$$SATURATION = 0.3 + \frac{R^2}{0.7}. \quad (3)$$

- d describes the yearly amplitude of the considered pixel in the NDVI-LST feature space, which is coded in the remaining component, intensity, darker colors corresponding then to small yearly amplitudes, and light colors to more important yearly amplitudes. Intensity is derived from d values using Eq. (4):

$$INTENSITY = d + 0.2. \quad (4)$$

Eqs. (2)–(4) have been determined by optimization of visual contrast between vegetation types.

5. Discussion and conclusion

Fig. 3 shows that the Yearly Land Cover Dynamics method captures the annual behavior of the vegetation as has been evidenced in previous studies. For example, Lambin and Ehrlich (1996) showed in their Fig. 3 the time trajectories in the NDVI-LST space for the main African biomes in both hemispheres. Due to differences in LST estimation and normalization, direct comparison cannot be carried out, however, similar behaviors can be evidenced for the same biomes in both cases. Evergreen rainforests have a low positive NDVI-LST slope as evidenced in Fig. 3a ($\theta \sim 15°$), with a short seasonality as evidenced in Fig. 3b ($d \sim 0.25$), and an annual behavior far from linear as evidenced in Fig. 3c ($R^2 \sim 0.3$). Transition woodlands and savannahs have a negative NDVI-LST slope, confirming the θ values obtained for

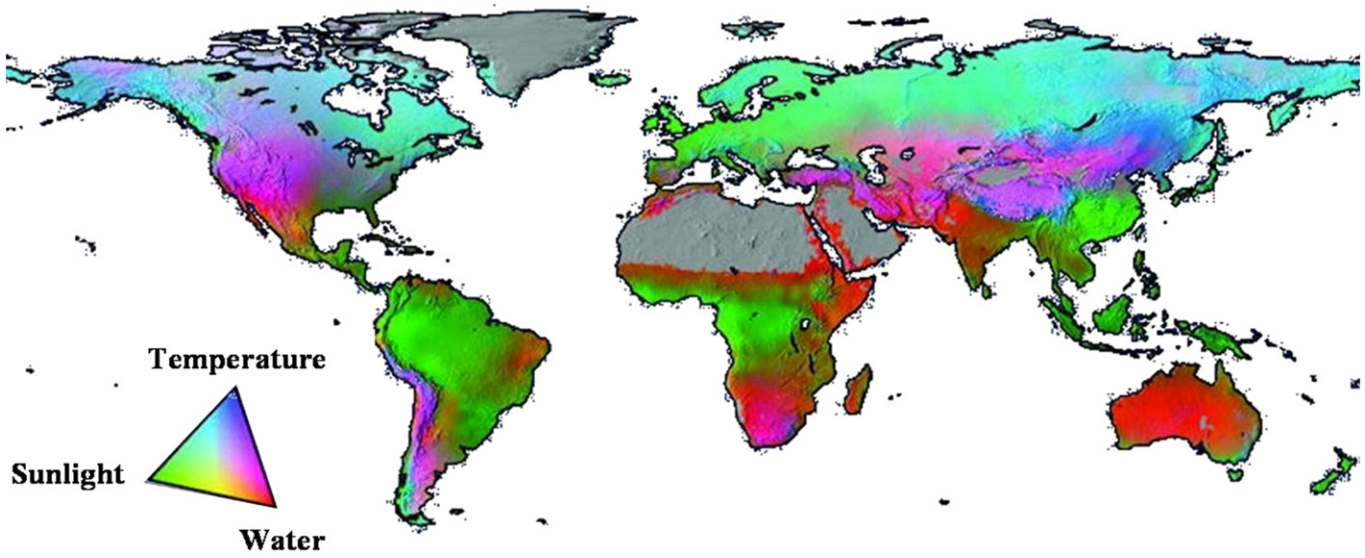

Fig. 5. Geographic distribution of potential climatic constraints to plant growth (adapted from Nemani et al., 2003). This map corresponds well with Fig. 4.

these biomes in Fig. 3a ($\theta \sim -30°$), with higher seasonality, as Fig. 3b confirms ($d \sim 0.5$), and an annual NDVI-LST pattern closer to the linear model (Fig. 3c: $R^2 > 0.6$). As for Sahel and Sahara regions, they show a quasi vertical NDVI-LST slope in Lambin and Ehrlich (1996), corresponding to the large negative θ values of Fig. 3a ($\theta < -45°$), with higher seasonality for the Sahara than for the Sahel region, mirrored in the d values presented in Fig. 3b ($d \sim 0.3$ and $d \sim 0.1$ respectively), and with an annual NDVI-LST pattern closer to the linear model for the Sahara ($R^2 \sim 0.4$) than for the Sahel region ($R^2 \sim 0.2$) as showed in Fig. 3c. Nemani and Running (1997) presented in their Fig. 2 a conceptual diagram showing the seasonal trajectories of different land cover types in the NDVI-LST space. This diagram is in agreement with Fig. 3, except for boreal evergreen forests, where Fig. 3b shows a higher seasonality than would be expected from their conceptual diagram. This is due to snow presence in the data during winter, which increases artificially the NDVI-LST yearly amplitude due to the low values of both NDVI and LST reached by vegetation covered by snow. As for the two methods presented in Sobrino and Raissouni (2000), displayed respectively in their Fig. 5 and 6, they were designed for the analysis of the desertification in arid and semi-arid areas. The method of the area of the triangle (MAT – Sobrino & Raissouni, 2000) is mirrored by the R^2 parameter of the YLCD method, which measures the difference between the linear model and the actual NDVI-LST annual pattern. A smaller triangle in the MAT method (bare soil) corresponds to a better adequacy with the linear model used in the YLCD method, and therefore a larger R^2 value, as can be verified in Fig. 3c. The method of the LST/NDVI slope (Sobrino & Raissouni, 2000) can be related directly to the θ parameter of the YLCD method, with lower negative values for bare soil than for vegetation in arid areas (water limited), as can be seen in Fig. 3a.

Fig. 4 shows that the YLCD method is well-suited for vegetation monitoring, since it allows a good description of the vegetation, in term of vegetation type as well as climate influence. Moreover, one has to keep in mind that this analysis has been carried out on an average year of orbital drift corrected data, meaning that cloud contamination and orbital drift influence have been greatly diminished. Determining NDVI-LST feature-space parameters with cloud contaminated yearly time series may lead for example to an artificial lengthening of the yearly cycle amplitude, as well as a wrong value of NDVI-$\hat{\text{LST}}$ regression line angle, and of course a lower value of R^2. Fig. 5 shows a global map of climatic constraints to plant growth published by Nemani et al. (2003). These climatic constraints are temperature, radiation and water. Visual comparison between Figs. 4 and 5 shows that the method presented above allows vegetation characterization including climatic constraints. As a consequence, this method seems promising for monitoring climate change effects on land cover. However, a quantitative validation of this method is needed, and will be carried out by the authors in a near future.

Additionally, the end products of this analysis (θ, d and R^2 parameters) are retrieved annually, and therefore can be monitored on a yearly basis. This monitoring may be achieved by statistical analysis or through building yearly classifications from existent AVHRR databases. Such work is currently under development within the Global Change Unit of the University of Valencia (Spain), and will hopefully increase our knowledge of the recent land cover changes suffered by our planet.

Acknowledgement

The authors wish to thank the European Union EAGLE project (SST3-CT-2003-502057) and the TERMASAT project (Ministerio de Educación y Ciencia, project ESP2005-07724-C05-04) for their financial support. The authors also wish to thank Molly E. Brown from the GIMMS group for providing the GIMMS data used in this work, as well as valuable information regarding these data.

References

Bayarjargal, Y., Karnieli, A., Bayasgalan, M., Khudulmur, S., Gandush, C., & Tucker, C. J. (2006). A comparative study of NOAA-AVHRR derived drought indices using change vector analysis. *Remote Sensing of Environment*, *105*, 9–22.

Borak, J. S., Lambin, E. F., & Strahler, A. H. (2000). The use of temporal metrics for land cover change detection at coarse spatial scales. *International Journal of Remote Sensing*, *Vol. 21*, 1415–1432 No. 6 & 7.

Clarke, T. R. (1997, January-March). An empirical approach for detecting crop water stress using multispectral airborne sensors. *Hort Technology*, *Vol. 7*(1).

Ehrlich, D., & Lambin, E. F. (1996). Broad scale land-cover classification and interannual climatic variability. *International Journal of Remote Sensing*, *17*(5), 845–862.

Gillies, R. R., Carlson, T. N., Cui, J., Kustas, W. P., & Humes, K. S. (1997). A verification of the 'triangle' method for obtaining surface soil water content and energy fluxes from remote measurements of the Normalized Difference Vegetation Index (NDVI) and surface radiant temperature. *International Journal of Remote Sensing*, *Vol. 18*, 3145–3166 No. 15.

Goetz, S. J. (1997). Multi-sensor analysis of NDVI, surface temperature and biophysical variables at a mixed grassland site. *International Journal of Remote Sensing*, *Vol. 18*, 71–94 No. 1.

Goward, S. N., Xue, Y., & Czajkowski, K. P. (2002). Evaluating land surface moisture conditions from the remotely sensed temperature/vegetation index measurements — An exploration with the simplified simple biosphere model. *Remote Sensing of Environment*, *79*, 225–242.

Holben, B. N. (1986). Characteristics of maximum values composite images from temporal AVHRR data. *International Journal of Remote Sensing*, *Vol. 7*, 1417–1434.

Hope, A., Engstrom, R., & Stow, D. (2005). Relation between AVHRR surface temperature and NDVI in Arctic tundra ecosystems. *International Journal of Remote Sensing*, *Vol. 26*, 1771–1776 No. 8.

Huete, A. R., Didan, K., Shimabukuro, Y. E., Ratana, P., Saleska, S. R., Hutyra, L. R., Yang, W., Nemani, R. R., & Myneni, R. (2006). Amazon rainforests green-up with sunlight in dry season. *Geophysical Research Letters*, *Vol. 33*, L06405. doi:10.1029/2005GL025583.

Huete, A. R., Liu, H. Q., Batchily, K., & van Leeuwen, W. (1997). A Comparison of Vegetation Indices over a Global Set of TM Images for EOS-MODIS. *Remote Sensing of Environment*, *Vol. 59*, 440–451 No. 3.

Julien, Y., Sobrino, J. A., & Verhoef, W. (2006). Changes in land surface temperatures and NDVI values over Europe between 1982 and 1999. *Remote Sensing of Environment*, *103*, 43–55.

Kidwell, K. B. (1998). *Polar orbiter data user's guide (TIROS-N, NOAA-6, NOAA-7, NOAA-8, NOAA-9, NOAA-10, NOAA-11, NOAA-12, NOAA-14)*. Washington D.C.: National Oceanic and Atmospheric Administration.

Lambin, E. F., & Ehrlich, D. (1996). The surface temperature-vegetation index space for land cover and land-cover change analysis. *International Journal of Remote Sensing*, *Vol. 17*, 163–487 No. 3.

Lambin, E. F., & Ehrlich, D. (1997). Land-cover changes in sub-Saharan Africa (1982–1991): Application of a change index based on remotely sensed surface temperature and vegetation indices at a continental scale. *Remote Sensing of Environment*, *61*, 181–200.

Nemani, R. R., Keeling, C. D., Hashimoto, H., Jolly, W. M., Piper, S. C., Tucker, C. J., Myneni, R. B., & Running, S. W. (2003). Climate-driven increases in global terrestrial net primary production from 1982 to 1999. *Science*, *Vol. 300*, 1560–1563.

Nemani, R. R., & Running, S. W. (1989). Estimation of regional surface resistance to evapotranspiration from NDVI and thermal-IR AVHRR data. *Journal of Applied Meteorology*, *Vol. 28*, 276–284.

Nemani, R. R., & Running, S. W. (1997). Land cover characterization using multitemporal red, near-IR, and thermal-IR data from NOAA/AVHRR. *Ecological Applications*, *7*(1), 79–90.

Nemani, R., Pierce, L., Running, S., & Goward, S. (1993). Developing satellite-derived estimates of surface moisture status. *Journal of Applied Meteorology*, *Vol. 32*, 548–557.

Sandholt, I., Rasmussen, K., & Andersen, J. (2002). A simple interpretation of the surface temperature/vegetation index space for assessment of surface moisture status. *Remote Sensing of Environment*, *79*, 213–224.

Schultz, P. A., & Halpert, M. S. (1995). Global analysis of the relationships among a vegetation index, precipitation and land surface temperature. *International Journal of Remote Sensing*, *Vol. 16*, 2755–2777 No. 15.

Sobrino, J. A., Julien, Y., Atitar, M. & Nerry, F., (2008). NOAA-AVHRR orbital drift correction from solar zenithal angle data, *IEEE Transactions on Geoscience and Remote Sensing, 46*(12), 4014–4019.

Sobrino, J. A., & Raissouni, N. (2000). Toward remote sensing methods for land cover dynamic monitoring: application to Morocco. *International Journal of Remote Sensing*, *Vol. 21*, 353–366 No. 2.

Tucker, C. J., Pinzon, J. E., Brown, M. E., Slayback, D. A., Pak, E. W., Mahoney, R., Vermote, E. F., & El Saleous, N. (2005). An extended AVHRR 8-km NDVI dataset compatible with MODIS and SPOT vegetation NDVI data. *International Journal of Remote Sensing*, *Vol. 26*, 4485–4498 No. 20.

Vermote, E., & Kaufman, Y. J. (1995). Absolute calibration of AVHRR visible and near-infrared channels using ocean and cloud views. *International Journal of Remote Sensing*, *Vol. 16*, 2317–2340 No. 13.

Wang, K., Li, Z., & Cribb, M. (2006). Estimation of evaporative fraction from a combination of day and night land surface temperatures and NDVI: A new method to determine the Priestley-Taylor parameter. *Remote Sensing of Environment*, *102*, 293–305.

Yue, W., Xu, J., Tan, W., & Xu, L. (2007). The relationship between land surface temperature and NDVI with remote sensing: Application to Shanghai Landsat 7 ETM+ data. *International Journal of Remote Sensing*, *Vol. 28*, 3205–3226 No. 15.